Received: 15 April 2021 | Revised: 5 July 2021 | Accepted: 8 July 2021

DOI: 10.1096/fj.202100638R

RESEARCH ARTICLE

THE FASEB JOURNAL

p53 regulation by MDM2 contributes to self-renewal and differentiation of basal stem cells in mouse and human airway epithelium

Sergio Garrido-Jimenez[1] | Juan Francisco Barrera-Lopez[1] | Selene Diaz-Chamorro[1] | Clara Maria Mateos-Quiros[1] | Ignacio Rodriguez-Blanco[2] | Francisca Lourdes Marquez-Perez[2] | Maria Jesus Lorenzo[1] | Francisco Centeno[1] | Angel Carlos Roman[1] | Jose Maria Carvajal-Gonzalez[1]

[1]Departamento de Bioquímica, Biología Molecular y Genética, Facultad de Ciencias, Universidad de Extremadura, Badajoz, Spain

[2]Departamento de Neumología, Hospital Universitario de Badajoz, Badajoz, Spain

Correspondence
Jose Maria Carvajal-Gonzalez, Departamento de Bioquímica, Biología Molecular y Genética, Facultad de Ciencias, Universidad de Extremadura, 06071-Badajoz, Spain.
Email: jmcarvaj@unex.es

Funding information
Ministry of Economy, Grant/Award Number: RYC-2015-17867, BFU2014-54699-P and BFU2017-85547-P; Junta de Extremadura, Grant/Award Number: IB18014 and GR15164; European Union FEDER program

Abstract

Proper physiological function of mammalian airways requires the differentiation of basal stem cells into secretory or multiciliated cells, among others. In addition, the self-renewal ability of these basal stem cells is crucial for developing a quick response to toxic agents in order to re-establish the epithelial barrier function of the airways. Although these epithelial missions are vital, little is known about those mechanism controlling airway epithelial regeneration in health and disease. p53 has been recently proposed as the guardian of homeostasis, promoting differentiation programs, and antagonizing a de-differentiation program. Here, we exploit mouse and human tracheal epithelial cell culture models to study the role of MDM2-p53 signaling in self-renewal and differentiation in the airway epithelium. We show that p53 protein regulation by MDM2 is crucial for basal stem cell differentiation and to keep proper cell proliferation. Therefore, we suggest that MDM2/p53 interaction modulation is a potential target to control regeneration of the mammalian airway epithelia without massively affecting the epithelium integrity and differentiation potential.

KEYWORDS
airway epithelial cells, MDM2, p53

1 | INTRODUCTION

The respiratory tract in mammals provides defense against inhaled pathogens and particles, such as cigarettes smoke or pollution. The airway epithelium lining this tract is composed of multiple cell types in mammals, including secretory cells (Club and Goblet cells), multiciliated cells (MCC), and basal stem cells (BSCs).[1-3] The consensus in the field is that BSCs are the progenitor cells for the rest of cell types during development, homeostasis, and regeneration, although their

Abbreviations: ALI, air-liquid interface; AOs, airway organoid; BSCs, basal stem cells; CCs, club cells; CF, cystic fibrosis; COPD, chronic obstructive pulmonary disease; GCs, goblet cells; MCC, multiciliated cells; MTECs, mouse tracheal epithelial cell culture; NSCLC, non-small cell lung cancer.

distribution along the airway differs among species.[4-6] In mouse, BSCs are only found in the main bronchi and trachea, whereas in humans they are distributed throughout the branching airway tree. Secretory cells provide mucus to trap pathogens and particles. In addition, club cells (CCs) also hold the potential to regenerate the epithelia as club progenitor cells.[7,8] To complete the airway epithelial basic function, MCCs employ their cilia beating to brush the mucus out of the organism and to keep dirt-free airways allowing a correct air flow.[9]

Proper functioning of this pseudostratified epithelia requires an adequate balance between all those different cell types. An imbalance in the abundance of BSCs or differentiated cell types, is seen in a variety of airway diseases such as asthma, chronic obstructive pulmonary disease (COPD), and cystic fibrosis (CF).[5,10] Nonetheless, the molecular pathways controlling proliferation and cell fate during both lung development and regeneration or during pathological states are still poorly understood. It is known that BSCs generate differentiated cells during postnatal growth and in the adult at steady state, although they are considered to be relatively quiescent. Nevertheless, BSCs retain their ability to respond rapidly to repair epithelial injury.[4] Important for regenerative biology and medicine, isolated BSCs are able to reconstitute the airway epithelia in culture conditions.[4,11]

The p53 homologs, p63 and p73, have been shown to play critical roles on the composition of the airway epithelium and therefore on its physiological function. p63 is highly expressed in BSCs of the airway epithelia and it is critical for maintaining this progenitor cell populations.[12,13] p63 null mice lack BSCs and die at birth with multiple organ abnormalities, including lung alterations.[12] On the other hand, p73 is enriched in MCCs, supporting its critical role for proper development and functioning of MCCs in the airway.[14] Mice with p73 deficiency suffer from chronic respiratory tract infections due to profound defects in ciliogenesis and complete loss of mucociliary clearance.[14] Molecularly, p73 chIP-seq experiments revealed that p73 orchestrates most of the MCC transcriptional network, including Foxj1, Rfx2, and Rfx3.[14,15]

The third member of this transcription factor family, p53, has been shown to play a role in club progenitor cells in the airway, but the role of p53, if any, in BSCs-mediated differentiation has not been clarified. As mentioned above, like BSCs, club progenitor cells are able to regenerate the airway epithelium under certain circumstances, but a de-differentiation process from club progenitor cells to BSCs is required.[16] Loss of p53 in club progenitor cells increases self-renewal, multipotency, and proliferation of BSCs derived from club progenitor cells. In a complementary experiment, an extra copy of *Trp53* promotes terminal differentiation and decreased proliferation of BSCs derived from club progenitor cells. Moreover, Jeong et al showed that inactivation of p53 promotes BSCs self-renewal in vitro, increasing the number of airway organoid (AO) formation, but p53 function on BSCs-mediated differentiation was not explored.[17]

In the present study, we investigate the function of p53 on BSCs homeostasis and differentiation. Using molecular and pharmacological approaches in mouse tracheal epithelial cell culture (MTECs) and human bronchial epithelial cells, we have found that p53 protein levels regulation is important to keep BSCs self-renewal and differentiation competence.

2 | MATERIALS AND METHODS

2.1 | Isolation of mouse tracheal epithelial cells (MTECs)

Mouse tracheal epithelial cells were isolated from wild-type C57BL/6J adult mice using the procedure reported by You et al[18] with minor modifications. Mice were sacrificed and tracheas were dissected from the bronchial main to the larynx and collected in cold Ham-F12 containing penicillin and streptomycin. After resection, vascular, fatty tissues, and muscle were removed in cold media. Clean tracheas were excised longitudinally and then incubated in Ham's F-12 pen-strep with 1.5 mg/mL of pronase (Roche Molecular Biochemicals) for 16 hours at 4°C. Afterward, fetal bovine serum (FBS, Gibco) was added to a final concentration of 10%. Processed tracheas were discarded, and the isolated cells were collected by centrifugation at 500 *g* for 5 minutes at 4°C. Then the cells were incubated for 10 minutes in F-12 medium containing 0.5 mg/mL pancreatic DNAse I (Sigma), and collected again by centrifugation. Finally, cells were seeded within PneumaCult-Ex Plus complete medium (StemCell) in primary tissue culture plates (Corning) for 4 hours in 5% CO_2 at 37°C to remove fibroblasts. Supernatant was collected, and MTECs were seeded in type I rat tail collagen (Gibco)-coated plates. We used a 60-mm plate for every three tracheas.

2.2 | Culture of mouse tracheal cells and treatments

MTECs were cultured in 5% CO_2 at 37°C, and PneumaCult-Ex Plus medium (StemCell) was replaced every 2 days until 70%-80% confluence (3-5 days after plating). Cells were then detached from plates by two consecutive incubations, with 0.02% EDTA in PBS for 5 minutes at 37°C, and accutase (Gibco) for 5 minutes at room temperature (RT). For MTECs differentiation, 9×10^4 cells/cm^2 were seeded in supported polyester porous membranes (Transwell 0.4 um pores, Corning). Upper and lower chambers were filled with PneumaCult-Ex Plus. Cells proliferated during 4-6 days with media in the upper chamber and lower chamber with expansion media. Once the epithelial monolayer reached

confluency, cells were switched to air-liquid interface (ALI). During ALI culture, PneumaCult-ALI Medium (StemCell) was maintained only in the lower chamber. An ALI was maintained until the end of the differentiation, 14 days (ALI 14). Samples in ALI 0 are those where we removed the media and processed the sample directly for ARN, protein, or any other assay. Samples in ALI 4, ALI7, and ALI14 are those that were expanded in the filters for 4-5 days in expansion media, once they reached confluency, we changed the media to ALI and keep them in ALI/differentiation media for 4, 7, or 14 days, respectively. Monolayer transepithelial electrical resistance (TEER) was measured during differentiation by an epithelial Ohm-voltmeter (EVOM3, WPI). For MDM2/p53 inhibition, either Nutlin-3a (sigma) 2 μM or AMG-232 (BioVision) 2.5 μM was added to the medium during expansion or differentiation of MTECs cultures (or in differentiated cells in the maintenance experiment), and dimethyl sulfoxide (DMSO) was used as a vehicle control. In the case of recovery experiments, DMSO was added in cells previously treated with Nutlin-3a or AMG-232 during differentiation process for 5 days and then keep them in a culture without treatment for 5 additional days.

2.3 | Isolation of human bronchial epithelial cells

The collection of human bronchial tissues was obtained by bronchoscopy from healthy donors in collaboration biobank of area de Salud de Badajoz with the approval of the accredited ethical committees that reviewed and approved the study in accordance to the law (BIOBANCO). Informed consent was obtained from all subjects. Samples and data from patients included in this study were provided by the Biobanco del Área de Salud de Badajoz (reference B.0001437) registered in the Spanish National Register and they were processed following the standard operating procedures with the appropriate approval of the Ethics and Scientific Committees. BRO 001 (Female aged 46) and BRO 002 (Male aged 30) samples were cleaned with PBS and incubated in Ham's F-12 pen-strep with 1 mg/mL of pronase (Roche Molecular Biochemicals), 0.5 mg/mL of pancreatic DNAse I, and 10 μM of Rock inhibitor (Y27632, Tocris) for 16 hours at 4°C. Isolated cells were collected by centrifugation at 500 *g* for 5 minutes at 4°C and resuspended in PneumaCult-Ex Plus complete medium (StemCell). Cells were seeded in primary tissue culture plates (Corning) for 4 hours in 5% CO_2 at 37°C to remove fibroblasts. Supernatant was collected, and bronchial epithelial cells were seeded in type I rat tail collagen (Gibco)-coated plates. Cells were cultured until 70%-80% confluence and we proceeded as described for MTECs. An ALI was maintained for human cells until 21 days (ALI 21).

2.4 | Culture of mouse and human airway organoids (AOs)

MTECs were expanded as described above, and when 60%-70% confluence was reached, cells were detached. Ninety-six-well plates were coated with 100 μL of 30% matrigel (Corning) in PneumaCult-Ex Plus medium (StemCell) and then incubated at 37°C for 20 minutes until its gelation. Five hundred MTECs in 100 μL of 2% matrigel in PneumaCult-Ex Plus were then seeded on top of the matrigel layer. For MDM2/p53 inhibition, 24 hours post-cell seeding Nutlin-3a and AMG-232 were added to the upper liquid medium at a concentration of 4 and 5 μM, respectively, and DMSO was used as vehicle control. To generate human organoids, human bronchial epithelial cells were cultured until 60%-70% confluence. Detached cells were resuspended in 100 μL of 2% matrigel in PneumaCult-Ex Plus and seeded on the top of 96-well coated with 100 μL of 30% matrigel. Airway organoids images were obtained after 5 days using an EVOS Floid Cell Imaging Station (Invitrogen).

2.5 | Lentivirus production and infection

Short hairpin RNAs (shRNAs) against p53 and MDM2 were inserted in the pLKO.1 vector, which drives the expression of shRNAs from the U6 human promoter and contains a puromycin resistance selection sequence. shRNA against luciferase was provided by Miguel Fidalgo. shRNAs were cloned using EcoRI and AgeI sites as described by Woo et al[19] (see, shRNA sequences listed in Table S1). Purified DNA was transfected together with the packaging vectors psPAX2 and PMD2.G into HEK-293T cells using polyethylenimine (PEI; Sigma). For the overexpression experiments, pLenti6/V5-p53 WT (Addgene 22945), pLenti6/V5-p53 R175H (Addgene 22936), and empty vector (control) were transfected in 293T instead of pLKO.1/shRNA. After 48 and 72 hours, viral supernatants were concentrated in Amicon Ultra-15 filters (Merck) by centrifugation at 3500 *g* for 30 minutes up to an approximate concentration of 2×10^5 infectious virus particles/mL. We added a volume of 75 μL of concentrated virus in 2 mL of medium in presence of 8 μg/mL of polybrene (Sigma) for a 60-mm plate. MTECs were selected after infection with a final concentration of 3 μM of puromycin during 48 hours before proceeding to the experiments.

2.6 | Western blot (WB) analysis

Cells were lysed in ice-cold lysis buffer containing 50 mM Tris-HCl (pH 7.5), 1 mM EGTA, 1 mM EDTA, 1 mM sodium orthovanadate, 5 mM sodium pyrophosphate, 10 mM sodium fluoride, 0.27 M sucrose, 0.1 mM phenylmethylsulphonyl

fluoride, 0.1% (v/v) 2-mercaptoethanol, 1% (v/v) Triton X–100, and complete protease inhibitor cocktail (Roche). Protein concentration was determined by Bio-Rad protein assay and 10 μg of protein was analyzed by SDS-PAGE electrophoresis and blotted onto nitrocellulose membranes (Bio-Rad Laboratories). The membranes were blocked with 5% dry milk Tris-buffered saline containing 0.05% Tween-20 before overnight incubation with primary antibodies at 4°C. Primary antibodies for WB were diluted in blocking solution. Antibodies used were anti-p53 (Cell signaling #2524, 1:1000), anti-MDM2 (Santa Cruz Biotechnologies #sc-965, 1:200), anti-P63 (Abcam #ab124762, 1:1000), anti-Cyclin D1 (Cell Signaling #2978), anti-vinculin (Sigma #V4505, 1:2000), and p53 posttranslational modification kit (Cell Signaling #37909, 1:1000). Membranes were washed with TBS-Tween and then incubated with horseradish peroxidase (HRP)-conjugated secondary antibodies (anti-rabbit-HRP, Cell Signaling #7074; anti-mouse-HRP, Cell Signaling #7076) in blocking solution (1:1000) for 1 hour at RT. After several washes with TBS-Tween, proteins were analyzed using a chemiluminescence detection system (SuperSignal West Dura, Thermo Fisher Scientific) and detected with iBright CL1000.

2.7 | RNA extraction, cDNA synthesis, qPCR, and RNA-Seq

Total RNA was extracted using illustra RNAspin Mini kit (GE Healthcare). After elution, 200-400 ng of RNA were reverse transcribed with High-Capacity cDNA Reverse Transcription Kit (Applied Biosystems) according to the manufacturer's instructions. Gene expression was analyzed by qPCR using oligonucleotides listed in Table S2 and Power SYBR Green PCR Master Mix (Applied Biosystems) instructions. Melt curve analyses were used to verify the specificity of the reactions. In the case of RNA-seq, samples were processed at the Service of Techniques Applied to Biosciences (STAB), in the University of Extremadura to generate libraries, and raw reads were obtained using Ion Torrent NGS technology. Afterward, the reads were aligned to the *Mus musculus* genome (mm10) using BWA, and transcript counts were normalized to TPM (Transcripts per Million mapped reads) scores using Express software, in order to be able to compare the gene expression across samples. Raw and processed data can be found at ArrayExpress (E-MTAB-8852).

2.8 | Scanning electron microscopy

Differentiated MTECs at ALI 14 were prepared for scanning EM by fixation with 2.5% glutaraldehyde for 90 minutes at 4°C, and then they were washed in 0.2 M cacodylate and finally stained with 1% osmium tetroxide (Sigma) in 0.2 M cacodylate for 2 hours at 4°C. Samples were dried by the technique of liquid carbon dioxide critical point, gold sputter coated, and visualized in a Quanta 3D FEG (ESEM-FIB; FEI Company).

2.9 | Immunofluorescence

MTECs cultures differentiated at ALI 14 were fixed in 4% formaldehyde (PolyScience) for 10 minutes at RT, permeabilized in 0.1% Triton for 10 minutes, and blocked with 2% bovine serum albumin (BSA, Roche) for 45 minutes. Samples were incubated with primary antibodies overnight at 4°C in the same blocking buffer. Primary antibodies used for immunofluorescence (IF) were anti-P63 (Abcam #ab124762, 1:200), MDM2 (Santa Cruz Biotechnologies #sc-965, 1:50), anti-P73 (Cell Signaling, #14620, 1:200), anti-FoxJ1 (Invitrogen, #14-9965-82, 1:200), anti-SCGB1a1 (Santa Cruz, #sc-9772, 1:100), anti-Muc5A/C (Invitrogen #MA5-12178), and anti-mCherry (Thermo #PA5-34974).. After this incubation, samples were washed five times in 0.1% Triton and then incubated for 1h with fluorescent secondary antibodies diluted in the same buffer. Secondary antibodies used for IF were Alexa Fluor 594 anti-Goat (Invitrogen, #A11058, 1:200), Alexa Fluor 594 anti-Rabbit (Invitrogen, #A11012, 1:200), Alexa Fluor 488 anti-Rabbit (Invitrogen, #A21206, 1:200), and Alexa Fluor 594 anti-Mouse (Invitrogen, #A11005, 1:200). To stain nuclei, DAPI was used at 0.5 μg/mL (Thermo Fisher Scientific, #62248). Five additional washes were performed in 0.1% Triton. Slides were mounted in Vectashield (Vector Labs) and images were obtained using an Olympus FV 1000 confocal microscope. After acquisition, images were processed using ImageJ (Fiji), and Adobe Photoshop CC 2018.

2.10 | Cell cycle, apoptosis, and senescence assay

For the quantitative evaluation of cell cycle and apoptosis, MTECs were treated with 2 μM Nutlin-3a, 2.5 μM AMG-232, or DMSO in PneumaCult-Ex Plus during 96 hours. Cell were then detached and stained with Annexin V-FITC (Invitrogen, 1:40 in binding buffer) for apoptosis measurement and with Hoechst-42 (Molecular Probes, 10 μg/mL) for the assessment of cell cycle. 1×10^5 cells were analyzed in MACSQuant X Flow cytometer (Miltenyi Biotec) and data were processed in Flowlogic software (Miltenyi Biotec). Finally, senescence of Nutlin-3a-treated cells during expansion (96 hours) and differentiation (ALI14) was measured using β-Gal staining kit (Cell Signaling Technologies) and β-Gal substrate C_{12}FDG (Invitrogen) according to the manufacturer's instructions. C_{12}FDG-positive cells were evaluated by flow cytometry.

2.11 | Cilia beating frequency measurement

Cilia beating frequency was measured in ALI14 MTECs treated with DMSO, Nutlin-3a, and AMG-232. The upper chamber of 12-mm transwells was incubated with 5 µL of Dynabeads Streptavidin C1 (Invitrogen) in 300 µL of Ca/Mg-PBS for 10 minutes at 37°C. After incubation, the medium from the upper chamber was removed and transwells were incubated for 90 minutes at 37°C. Before movie recording, 100 µL of Ca/Mg-PBS at 37°C was added on top of the transwell. Cilia beating movie was obtained using Motic AE20 microscope and an iPhone X at 240 fps, and a custom MATLAB function was developed to assess the movement of the beads as well as to quantify the cilia beating frequencies using FFT.

2.12 | MTECs monolayer integrity assay

To evaluate the monolayer integrity of MTECs culture, transwells treated with MDM2 inhibitors and DMSO at ALI14 were washed two times with cold Ca/Mg-PBS followed by two 20 minutes incubations at 4°C with 2 mg/mL of Sulfo-NHS-LC-Biotin (Thermo Scientific) in the upper chamber of the transwell. Cells were then fixed during 30 minutes with 4% paraformaldehyde and stained with Alexa Fluor 555 Streptavidin (Invitrogen, 1:500), 0.5 µg/mL DAPI and Alexa Fluor 488 phalloidin (Invitrogen, 1:500). Slides were mounted in Vectashield and images were obtained using an Olympus FV 1000 confocal microscope. After acquisition, images were processed using ImageJ (Fiji), and Adobe Photoshop CC 2018.

2.13 | Single-cell RNA-seq analysis

We used the GSE102580 dataset[20] from NCBI GEO in order to analyze the cell-type expression of specific genes in mouse and human airway epithelia. A custom MATLAB function was developed in order to generate a dot plot showing average expression and cell percentage.

2.14 | Statistical analyses

Data were analyzed using two-tailed *t* tests to compare control conditions with different experimental groups (GraphPad Prism). The n value in figure legends for WB and qPCR represents independent samples which are single transwells coming from at least three differentiation sets. In qPCR experiments, each independent sample is the average of 2-3 technical replicates. n values for IF are images or single nucleus.

3 | RESULTS

3.1 | Levels of p53 protein and its regulator MDM2 vary along the differentiation process of mouse tracheal epithelial cells

Isolation of BSCs from mammals and their in vitro differentiation using 2D (MTECs, mouse tracheal epithelial cells) cultures in ALI or 3D (Airway organoids (AOs)) cultures with extracellular matrix,[21] have been proved to be an excellent up-to-date model system to study the proximal airway biology.[20,22,23] Using the former model system, we first monitor mRNA expression levels of p53 along the differentiation process of BSCs in vitro. As showed in Figure 1, p53 mRNA levels remained un-variable/constant in early stages of the differentiation process, between days 0, 4, and 7 of differentiation (ALI 0, ALI 4, and ALI 7) (Figure 1A). From ALI 0 to ALI 7, differentiation markers for MCCs and secretory cells started to appear from ALI 4 to ALI 7 (Figure S1E-G). Next, we monitored the p53 family member at the protein level from ALI 0 to ALI 14. Surprisingly, we found that p53 protein levels showed an increase at day 4 of differentiation (Figure 1C,D). As expected, p63 reduced its expression at ALI 14 (most likely due to a reduction in the proportion of BSCs) (Figures 1C and S1) and p73 was enriched in MCC as previously published (Figure S1I). Altogether, our data suggest that a protein stabilization process instead of a transcriptional regulation was in place for p53 during differentiation of BSCs in 2D cultures. It could be also the case that p53 expression was, like p63 or p73, ligated to a specific cell type.

p53 protein levels are tightly regulated by MDM2 (murine double minute 2). The E3 ubiquitin ligase MDM2 is an oncoprotein that ubiquitinates and target for degradation proteins including p53 among many others.[24-26] Closing a negative feedback loop, p53 also regulates MDM2 expression.[27] Based on this information, we tested MDM2 mRNA levels and protein levels in our experimental conditions from ALI 0 to ALI 14. We found that MDM2 mRNA levels decreased at ALI 4 and ALI 7 (Figure 1B), while its protein levels are dramatically reduced at the beginning of this BSCs differentiation process (Figure 1C,E). We also determined the expression levels of other seven E3 ubiquitin ligases (Trim28, Trim24, Arf-BP1, Rnf6, Chip, Cop1, and Pirh2) and found that only Pirh2 and Rnf6 decreased the expression along the differentiation process similar to MDM2 (Figure S1G-M). Looking at published single-cell RNA-seq data at steady state, we found that MDM2 expression is higher and enriched in murine MCCs, while p53 is more homogeneously expressed in all different airway epithelial cell types (Figure S1N). Like p53, we also found that the other p53-related E3 ubiquitin ligases were homogeneously expressed in all cell types in the airway (Figure S1M). Thus, our data indicate that MDM2 may play a role at early stages of differentiation (ALI

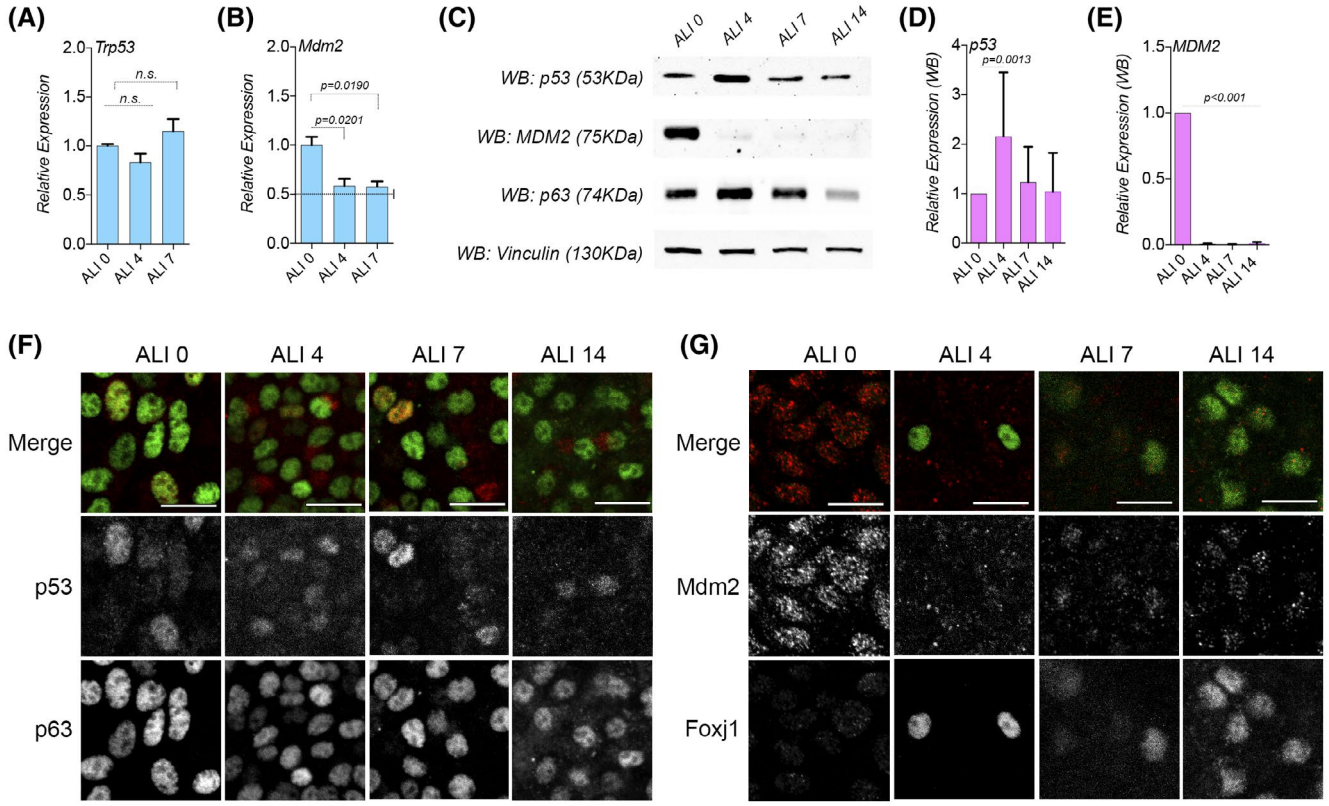

FIGURE 1 p53 protein levels varies along the differentiation process of airway epithelial cells culture in vitro. A,B, *Trp53* and *Mdm2* mRNA expression levels in ALI 0, ALI 4, and ALI 7. C, Western blots images for p53, MDM2, and p63 protein levels assayed during the differentiation process at ALI 0, ALI 4, ALI 7, and ALI 14. Vinculin was also assayed as a loading control. D,E, Western blots quantification for p53 and MDM2 were normalized using Vinculin as a loading control and then all values for each differentiation set were made relative to ALI 0 values. Mean and standard deviation as error bars were plotted for each protein and differentiation time point, n = 7. F, p53 protein localization in the epithelial monolayer along the differentiation, from ALI 0 to ALI14, process relative to p63-positive cells. G, MDM2 protein localization along the differentiation in the epithelial monolayer, from ALI 0 to ALI 14, relative to Foxj1. Scale bar in F and G represents 20 μm. *P* values in all conditions were obtained using two-tailed *t* test

0-ALI 7) of BSCs regulating p53 protein levels, but we cannot discard the role of other p53-related E3 ubiquitin ligases during differentiation of BSCs.

To study the role of p53 and MDM2 in BSCs differentiation, we tested by IF the localization of p53 and MDM2 in the airway cultures along the differentiation process. For p53, we detected its expression in most of the p63-positive cells (BSCs) in ALI 0. In ALI 4 and ALI 7, p53 is not only expressed in p63 cells but it also appeared in p63-negative cells. Finally, in ALI 14 we do not find p53 in p63-positive cells but p53 is expressed at low levels in other cells types (Figures 1F and S2A). In the case of MDM2, we detected a strong signal in all the cells in ALI 0 (BSCs). In ALI 4, MDM2 is completely depleted, although we started to detect few Foxj1-positive cells which are negative for MDM2. In ALI 7 and ALI 14, we detected MDM2 signal only in Foxj1-positive cells (Figures 1G and S2B).

Based on this experimental characterization, we concluded that p53 and MDM2 expression varied along the differentiation of BSCs. This variation is related to the protein expression levels but also to the appearance of different cell types.

3.2 | p53 and MDM2 protein levels modulation affects BSCs differentiation

The next step was to assess if p53 or MDM2 is required for proper BSCs differentiation. To answer this, we developed a knockdown protocol for p53 in BSCs using shRNA (Figure 2A-C). As shown in Figure 1, p53 protein levels were reduced above 80% in 96 hours post-infection of BSCs (Figure 2A,B) and above 90% of cells incorporated the shRNA vector in ALI 14 (around 20 days post-infection) (Figure S3). BSCs were infected with shRNA against luciferase (Luc, as control) or three validated shRNAs for p53 and tested for different airway epithelium cell types with IF. To our surprise, p63-positive cells number were the same between control or p53-KD cells (Figure S3C,D), and Scgb1a1-positive cells were mildly

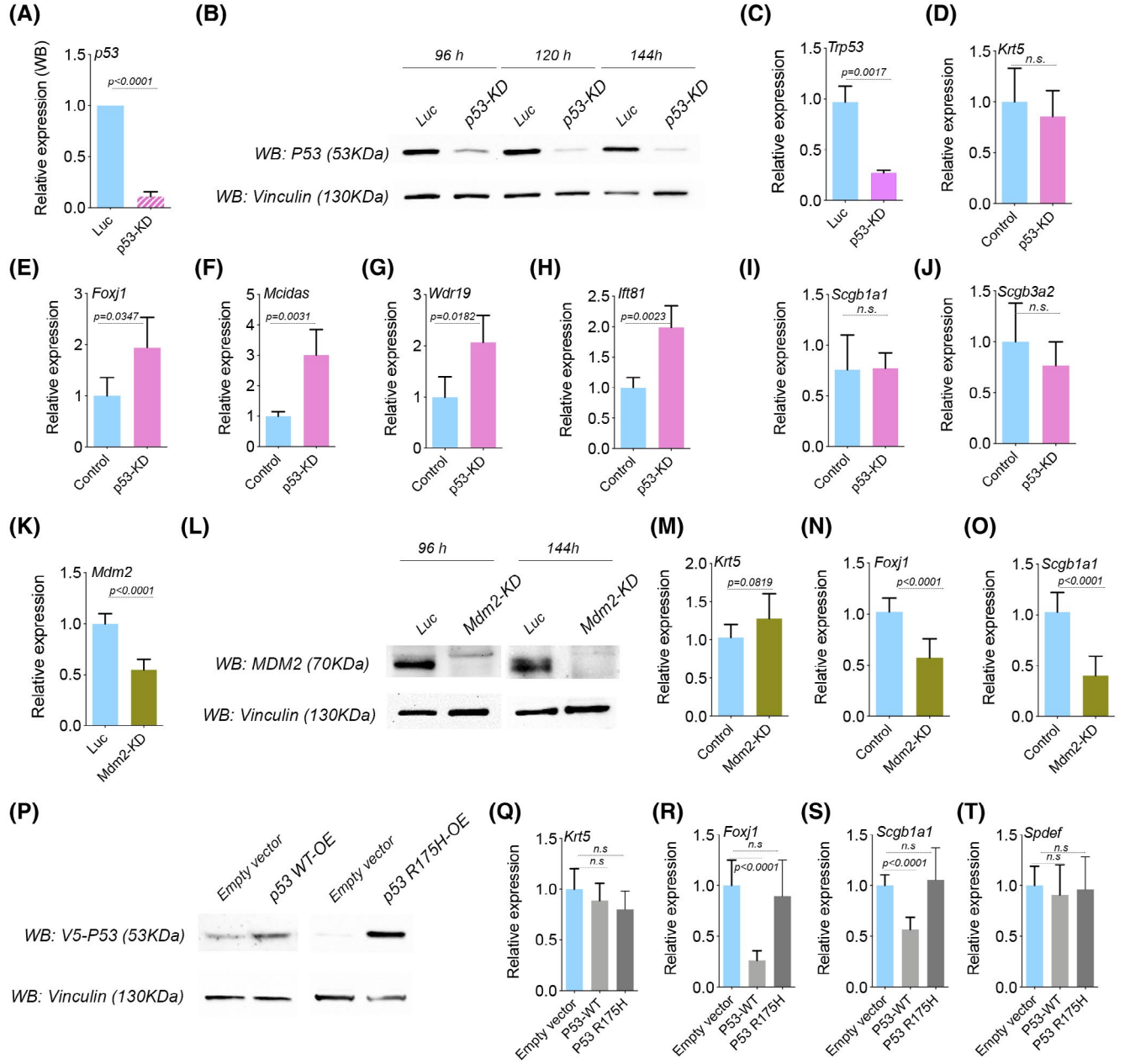

FIGURE 2 p53 protein levels varies along the differentiation process of airway epithelial cells culture in vitro. A, Quantification of p53 protein levels in p53-KD compared to control. Values were normalized and made relative to control conditions. Bars represent the mean of expression in each condition and error bars represent the standard deviation, n = 9. B, Western blots images in MTECs with knockdown of p53 at 96, 120, and 144 hours post-infection. C, Mean mRNA expression levels of p53 assed in differentiated MTECs infected with control viruses (Luc) or p53-shRNAs (p53-KD), n = 3. I, Representative images for control and p53-KD cells processed for immunofluorescence to evaluate different cellular linages. Antibodies for p63, Foxj1, or Scgb1a1 were used for basal cells, MCCs, and club cells, respectively. Expression levels in Luc vs p53-KD of MCCs markers, Foxj1, Mcidas, Wdr19, and IFT81 (M), club cells (Scgb1a1 and Scgb3a2) (N), and Krt5 for basal cells (O). Mean relative to control cells and standard deviation as error bars were plotted for each lineage marker, n = 4. K, Mean mRNA expression levels of MDM2 assed in differentiated MTECs infected with control viruses (Luc) or Mdm2-shRNAs (Mdm2-KD), n = 6. L, Western blots images in MTECs with knockdown of MDM2 at 96 and 144 hours post-infection. M-O, mRNA expression levels in Luc vs Mdm2-KD of Krt5 for basal cells (M), Foxj1 for MCCs (N), and Scgb1a1 for club cells (O). Mean relative to control cells and standard deviation as error bars were plotted for each lineage marker, n = 4. P, Western blots images for V5, a tag used to label the overexpressed p53 (WT or mutant R175H). Vinculin was used as a loading control. (Q-R) mRNA expression levels in control cells vs p53 WT overexpressing cells or p53 R175H overexpressing cells of Krt5 for basal cells (Q), Foxj1 for MCCs (R), Scgb1a1 for club cells (S), and Spdef for goblet cells (T). Mean relative to control cells and standard deviation as error bars were plotted for each lineage marker, n = 8. *P* values in all conditions were obtained using two-tailed *t* test

reduced in p53-KD cells (Figure S3C,F). However, the MCCs labeled with Foxj1 were increased in p53-KD cells when compared to control conditions (Figure S3C,E). To confirm these data, we measured the gene expression levels for specific cell type markers. We used Krt5 for BSCs and secretoglobins Scgb1a1 and Scgb3a2 for CCs. We did not find changes in expression between control and p53-KD cells for Krt5, Scgb1a1, or Scgb3a2 (Figure 2D,I,J). However, we corroborated the increase in MCCs in p53-KD conditions with four different MCCs markers (Figure 2E-H).

To test whether Mdm2 could affect BSCs differentiation to the different airway cell types or only MCCs differentiation; we successfully established the same knockdown approach used for p53, we used three shRNA against MDM2 (Figure 2K,L). Once MDM2 knockdown was confirmed by qPCR and WB, we compared the gene expression levels for BSCs, MCCs, and CCs cell types markers between control and Mdm2-KD cells. We found that knockdown of Mdm2 decreased the expression of Foxj1 and Scgb1a1 without an effect in Krt5 (Figure 2M-O).

In order to strengthen our data on Mdm2, we directly overexpressed p53-WT in BSCs (Figure 2P) and placed them for differentiation. After 14 days in ALI, we found that p53-WT decreased Foxj1 expression and Scgb1a1 (Figure 2R,S) and we did not detect significant differences in Spdef or Krt5 (Figure 2Q,T). Then as expected, p53-WT overexpression mimicked the effect of MDM2 downregulation. In a parallel experiment, we overexpressed a p53 mutant (R175H) (Figure 2P), with deficient ability to produce the transcriptional response of p53.[28,29] In this case, we did not find changes in the expression of Krt5, Foxj1, Scgb1a1, or Spdef (Figure 2Q-T), suggesting a transcriptional function of p53 during differentiation.

p53 transcription factor has been extensively studied and a meta-study identified 350 p53 putative gene targets.[30] We reasoned that if p53 transcriptional function is active during these early stages of differentiation, then some of those putative targets should vary their expression levels. As shown in Figure S1, we found that the above 15% of those p53 gene targets double or reduce to half their expression from ALI 0 to ALI7 (Figure S3I). This value falls within the range of the percentage of genes found in the single studies used for the p53 meta-analysis.[30] In addition, we found that p53 is phosphorylated in ALI0 in Ser9, Ser15, and Ser 46, located at the transactivation domain of p53 and supporting the active transcriptional role of p53 in early stages of differentiation (Figure S3J). Furthermore, p53 Ser 392 is also heavily phosphorylated and low acetylation levels were detected in Lys 376 (Figure S3J).

Overall, our findings support an active function of the MDM2/p53 pathway during early stages of BSCs differentiation.

3.3 | MDM2 regulates p53 protein levels during BSCs differentiation

The enrichment of MDM2 in MCCs together with the increase of MCCs in p53-KD cells and the decrease of MCCs in Mdm2-KD cells could support a tight regulation of the MDM2/p53 pathway in the differentiation of BSCs at least to MCCs. To study whether p53 protein levels could directly be regulated by MDM2 during BSCs differentiation, we targeted the MDM2/p53 interaction using two well-established MDM2 inhibitors, Nutlin-3a and AMG232. Nutlin-3a is a potent and selective small-molecule inhibitor of the MDM2/p53 interaction.[31] Nutlin-3a binds to the p53 binding site on MDM2. A similar competitive mechanism was described for AMG232.[32,33] Nutlin-3a and AMG232 do also have the ability to increase the expression of MDM2.[31,32] After 14 days of differentiation (ALI 14), shRNA treatment of BSCs reduced p53 protein levels and Nutlin-3a in WT cells increased p53 levels (Figure 3A,B). We also found that in p53-KD cells Nutlin-3a treatment recovered p53 protein levels above the normal ones (Figure 2A,B), although p53 mRNA levels were downregulated (Figure S4). Of note, this p53 modulation affected p73 and p63 expression levels after p53 was knocked down (Figure S4) and MDM2 protein levels were elevated in all conditions when compared to WT levels (Figure 3A,C). Once the system was settled to modulate p53 protein, we first evaluated the differentiation process using qPCR with specific markers for each cell type (we added *Spdef* expression as a gene marker for Goblet cells). Using Nutlin-3a or AMG232 treatment we found a reduced expression of MCC, CCs, and GCs cell type markers without a dramatic effect on Krt5 expression (except for Luc AMG 232 condition) (Figure 3D-G). A decrease in *Spdef* expression was also observed in Mdm2-KD cells (Figure S3). Next, we confirmed these data using IF using antibodies against p63, Foxj1, Scgb1a1 (Figures 3 and S4), and MUC5AC (Figure S4). Nutlin-3a and AMG232 reduced the number of Foxj1- and Scgb1a1-positive cells, while MUC5AC-positive cells were not detected when compared to WT conditions (Figures 3 and S4). We did not find a consistent increase or decrease in p63-positive cells in Nutlin-3a or AMG232-treated cells (Figures 3 and S4).

From previous lineage-tracing studies in the trachea, we know that Krt5-positive basal cells are the progenitors of secretory cells, which in turn give rise to MCCs.[4] BSCs continuously provide Notch ligand to their daughter secretory cells, without this signaling secretory cells suffer terminal differentiate to MCC.[34] To further confirm that MDM2/p53 regulates MCCs differentiation from BSCs, we treated cells with DAPT, a Notch signaling pathway inhibitor, in combination with AMG232 or Nutlin-3a. As expected, DAPT treatment of BSCs during differentiation blocked differentiation to CCs and increased BSCs and MCCs (Figures 3I-L and S4). The combination of inhibitors showed a decrease of

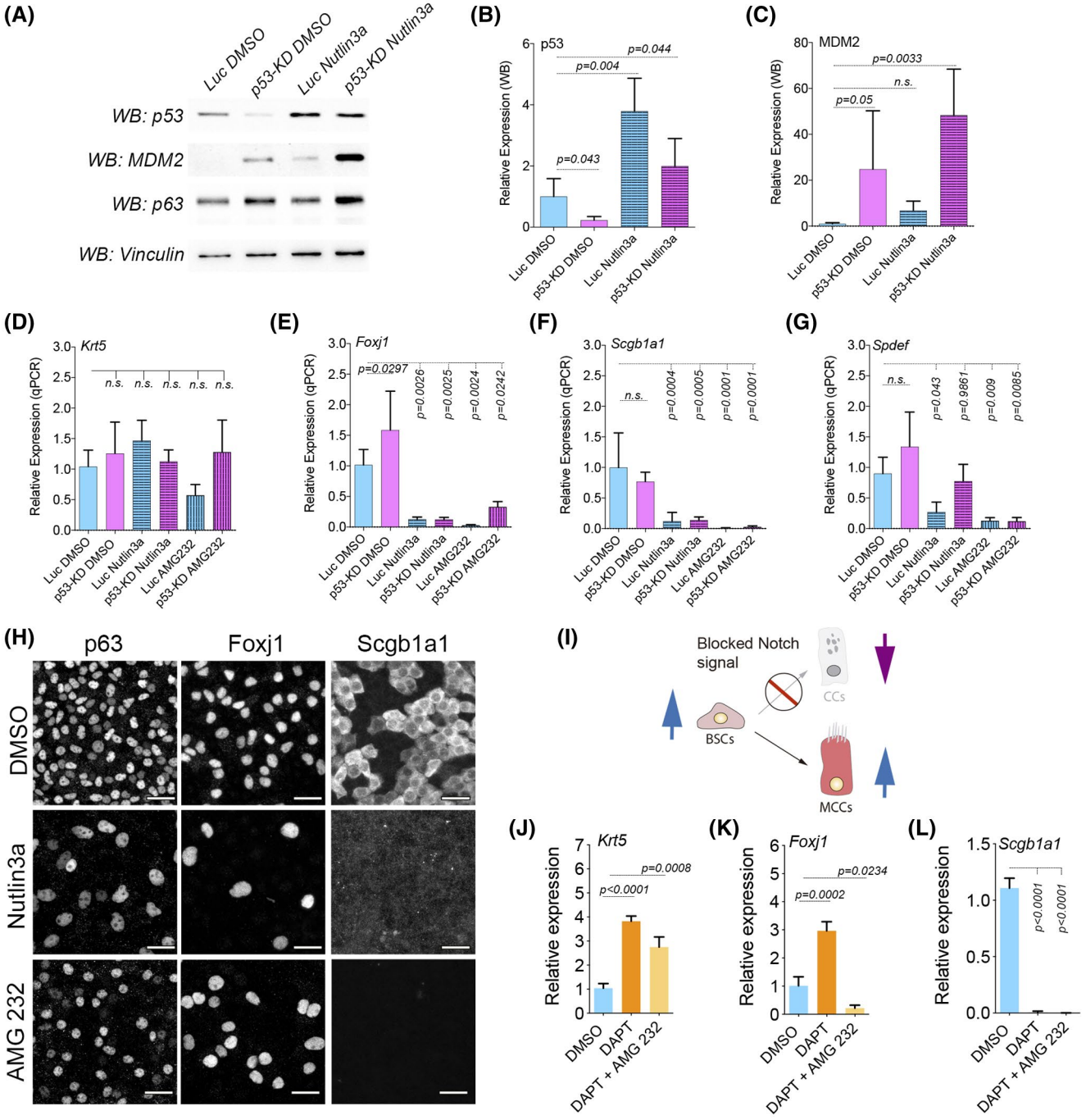

FIGURE 3 p53/MDM2 interaction modulation alters BSCs differentiation. A, Western blots images for p53, MDM2, p63, and vinculin in control (Luc) or p53-KD MTECs treated with Nutlin-3a or DMSO for 14 days. B,C, Quantification of WB for p53 (B) and MDM2 (C). Vinculin was used as a loading control and then all values for each differentiation set were made relative to Luc DMSO. Mean and standard deviation as error bars were plotted for each protein, n = 4. D-G, mRNA expression levels in Luc vs p53-KD treated with DMSO, Nutlin-3a, or AMG232 of Krt5 for basal cells (D), Foxj1 for MCCs (E), Scgb1a1 for club cells (F), and Spdef for goblet cells (G). Mean relative to control cells and standard deviation as error bars were plotted for each lineage marker, n = 7. H, Representative images for control and p53-KD cells treated with DMSO, Nutlin-3a, or AMG232 processed for immunofluorescence to evaluate the basal cells, MCCs, and club cells. I, Representative scheme for Notch inhibition expected phenotype. Notch signaling inhibition blocks BSCs differentiation toward club cells but induces MCCs differentiation and accumulation of BSCs. J-L, mRNA expression levels of Krt5 for basal cells (J), Foxj1 for MCCs (K), and Scgb1a1 for club cells (L) in MTECs treated with DMSO, DAPT, or DAPT/AMG232. Mean expression values relative to DMSO-treated cells and standard deviation as error bars were plotted for each lineage marker, n = 6. Scale bar in H represents 20 μm. *P* values in all conditions were obtained using two-tailed *t* test

MCCs and CCs, but retained the increase of BSCs induced by Notch inhibition (Figures 3I-L and S4). We also found that DAPT itself increased the expression of MDM2 and p53, which might represent a change in the representation of cell types (Figure S4).

Altogether this dataset confirmed that MDM2 regulation of p53 antagonizes BSCs differentiation to MCCs, CCs, and GCs without an apparent effect on BSCs. In addition, p53 directly blocks BSCs differentiation to MCCs.

3.4 | p53 protein level modulation affects the cell density but does not disturb the monolayer integrity

We noticed that nuclei labeled with p63 or Foxj1 were bigger when Nutlin-3a or AMG232 was applied compared to control DMSO conditions (Figure 3H). To further confirm this observation, we stained the nuclei with DAPI and then measured the nucleus size and density. As a result, we found that both Nutlin-3a and AMG 232 treatment increased nucleus size and decreased their density (Figure 4A-C). This same phenotype has been previously described in airway epithelial cell monolayers with an extra copy of *Trp53* (Super p53 mice) derived from club progenitor cells. We did not observe nucleus size or density changes in p53-KD cells (Figure 4A-C).

Since nucleus density could indicate that cell density was reduced and that the epithelial monolayer might be compromised, we conducted an experiment to test if those epithelial monolayers kept their integrity as a barrier. We biotinylated alive epithelial monolayers in ALI14 from the apical surface using non-permeable biotin, which can react with the exposed extracellular domains of plasma membrane proteins.[35,36] As we have previously shown with other 2D epithelial model systems like MDCK cells, epithelial monolayers with complete confluence and proper tight junctions should show surface biotinylation, detectable with fluorescence streptavidin, only at the apical side of the monolayer.[35] On the contrary, those monolayers with compromised integrity should show surface biotinylation at both the apical and the basolateral sides. As shown in Figure 4, MDM2 inhibitors do not affect the epithelial monolayer barrier function showing streptavidin labeling only at the apical surface like untreated cells (Figure 4D). Therefore, epithelial integrity was not compromised in MTECs treated with either Nutlin-3a or AMG232. To further analyze the monolayer barrier function and tight junction status, we directly measured transepithelial resistance (TEER) in the same experimental conditions. We found that p53-KD or Nutlin-3a-treated monolayers displayed the same TEER that control cells, but AMG232 cells had a dramatic increase in TEER (Figure 4E). Furthermore, MDM2-KD does not affect TEER (Figure S3). In sum, although cell density is compromised upon MDM2 inhibition, the epithelial monolayers retained its barrier function.

We also found that although CCs were almost totally absent, Foxj1-positive cells remained in both, Nutlin-3a- and AMG232-treated cells (Figure 3H). To closely observe those MCCs and their cilia, we used scanning electron microscopy (SEM) and found that cells treated with the MDM2/p53 interaction antagonists displayed shorter cilia in Nutlin-3a treatment and uneven cilia formation under AMG 232 treatment (Figure 4F). Surprisingly, cilia beating frequency was not affected in those MCCs developed in MTECs treated with Nutlin-3a when compared to DMSO-treated cells (Figure 4G). We found a mild defect, 1.6 beats less per second, in MCCs obtained in AMG232 conditions (Figure 4G).

Altogether our data demonstrate that p53 affects cell density but do not disturb the monolayer integrity, and that MDM2/p53 interaction is crucial for proper cilia development.

3.5 | Nutlin-3a-induced phenotypes are completely reversible but do not affect the cells once differentiated

Next, we asked whether BSCs treated with Nutlin-3a could fully differentiate upon drug removal, which we called phenotype recovery (Figure 5A), and if once differentiated MDM2/p53 interaction inhibition could affect already differentiated cultures, which we named phenotype maintenance (Figure 5H). For the MTECs recovery assay, we treated BSCs in ALI for 14 days with Nutlin-3a or DMSO (control) and then removed or kept those treatments for 14 additional days in ALI (Figure 5A). With those experimental conditions, we found that upon Nutlin-3a removal, cell type marker levels fully recovered to WT conditions (Figure 5B-D). In IF, p63-, Foxj1-, and Scgb1a1-positive cells were more abundant when compared to Nutlin-3a-treated cells for 28 days (Figure 5E) and nuclei DAPI staining analyses showed a reversal in size (Figure 5F). Similar phenotypes were observed in a parallel recovery experiment with AMG232 treatment (Figure S5). Furthermore, in scanning electron microscopy micrographs, Nutlin-3a- or AMG232-treated cells for 28 days MCCs displayed cilia with comparable morphology and abundance when compared to DMSO-treated cells for 28 days (Figures 5G and S5). In the phenotype maintenance experiment, we found that Nutlin-3a treatment after cell differentiation do not affect the expression of the different cell types markers after 14 days of treatment (ALI 28) (Figure 5H-K). However, we observed a significant increase in nucleus size without an effect in TEER (Figure 5L-M). In a closer look to the monolayer

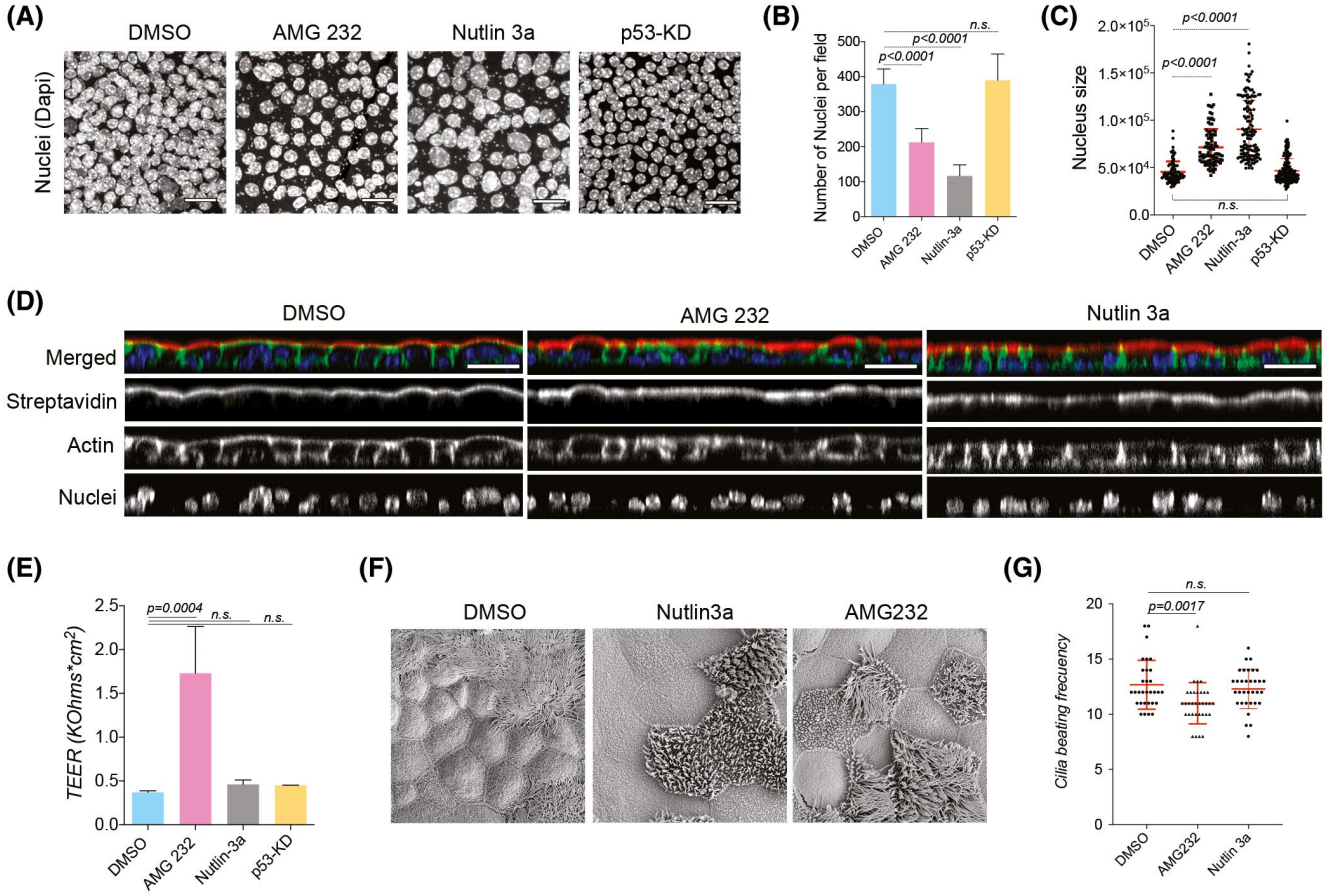

FIGURE 4 p53 protein levels modulation affects the cell density but does not disturb the monolayer integrity. A, DAPI staining images used to study the nucleus in differentiated MTECs treated with DMSO (control), AMG232, Nutlin-3a, or p53-KD. B,C, Nuclei density (n = 8) and nucleus size quantification (n > 200) in DMSO, AMG232, Nutlin-3a, or p53-KD experimental conditions. D, Confocal images corresponding to orthogonal views in MTECs treated with DMSO, AMG232, and Nutlin-3a. Differential labeling with biotin (only applied to the apical surface) was used to evaluate MTECs monolayer integrity upon Nutlin-3a or AMG232 treatment. Streptavidin Alexa Fluor 555 (in red) was only observed at the apical membrane. Actin (in green) was used to label the cortical actin in both, the apical and the basolateral surfaces. E, Transepithelial electrical resistance (TEER) of MTECs treated with DMSO, Nutlin-3a, or AMG232 and p53-KD (n = 8). F, Scanning electron micrographs of MTECs treated with DMSO, Nutlin-3a, or AMG232. G, Cilia beating frequency quantification as number of beats per second in cells treated with DMSO, Nutlin-3a, or AMG232 (n = 30-50). Scale bar in A and D represent 20 μm. *P* values in all conditions were obtained using two-tailed *t* test

by SEM we observed that Nutlin-3a treatment caused an increase in cell size and no major phenotypes in cilia morphology (Figure 5N).

Overall, this set of experiments confirmed that MDM2/p53 interaction is important during cell differentiation; however, these phenotypes are, to a large extend, reversible. Interestingly, Nutlin-3a treatment for 14 days does not provoke a massive effect on the airway epithelial monolayer once the monolayer achieved the steady state.

3.6 | MDM2/p53 regulates BSCs self-renewal and cell cycle

Classical p53 functions include cell cycle arrest, apoptosis, senescence, or quiescence.[37] Recently, p53 has been revealed to regulate stem cell function where p53 can suppress reprogramming due to arrest on cell cycle or induction of apoptosis.[38] A general view in stem cell biology is that p53 inhibits self-renewal and promotes differentiation.[39]

To test whether p53 could influence the proliferative state of BSCs without a differentiation stimulus, we assessed BSCs doubling time in control or p53-KD cells treated or not with Nutlin-3a. We found that p53-KD or Nutlin-3a treatment increased significantly the doubling time of BSCs (Figure 6A), suggesting an effect on proliferation, hence on self-renewal. To further confirm these phenotypes, we evaluated more directly self-renewal using AOs formation prior to cell differentiation.[4] We found similar phenotypes in AOs formation, p53-KD, and Nutlin-3a treatment arrested AOs growth when compared to control conditions (Figure 6C,D). Importantly, the percentage of AOs developed was not affected in p53-KD cells but was

dramatically affected in Nutlin-3a-treated cells (Figure 6B). In agreement with the Nutlin-3a data, MDM2-KD decreased AOs size and number (Figure S6). Moreover, Nutlin-3a-induced phenotype in AOs growth was also reversible suggesting that Nutlin-3a treatment does not induce substantial cell death (Figure S5). When p53 overexpression was assessed, WT or R175H, we did not detect significant changes in the percentage of AOs formation (Figure 6F) or size (Figure 6G). Indeed, we did not find changes in doubling time in those p53 overexpressing conditions (Figure S6).

Next, we evaluated cell cycle, apoptosis, and senescence in BSCs in control and p53-KD cells, treated or not with

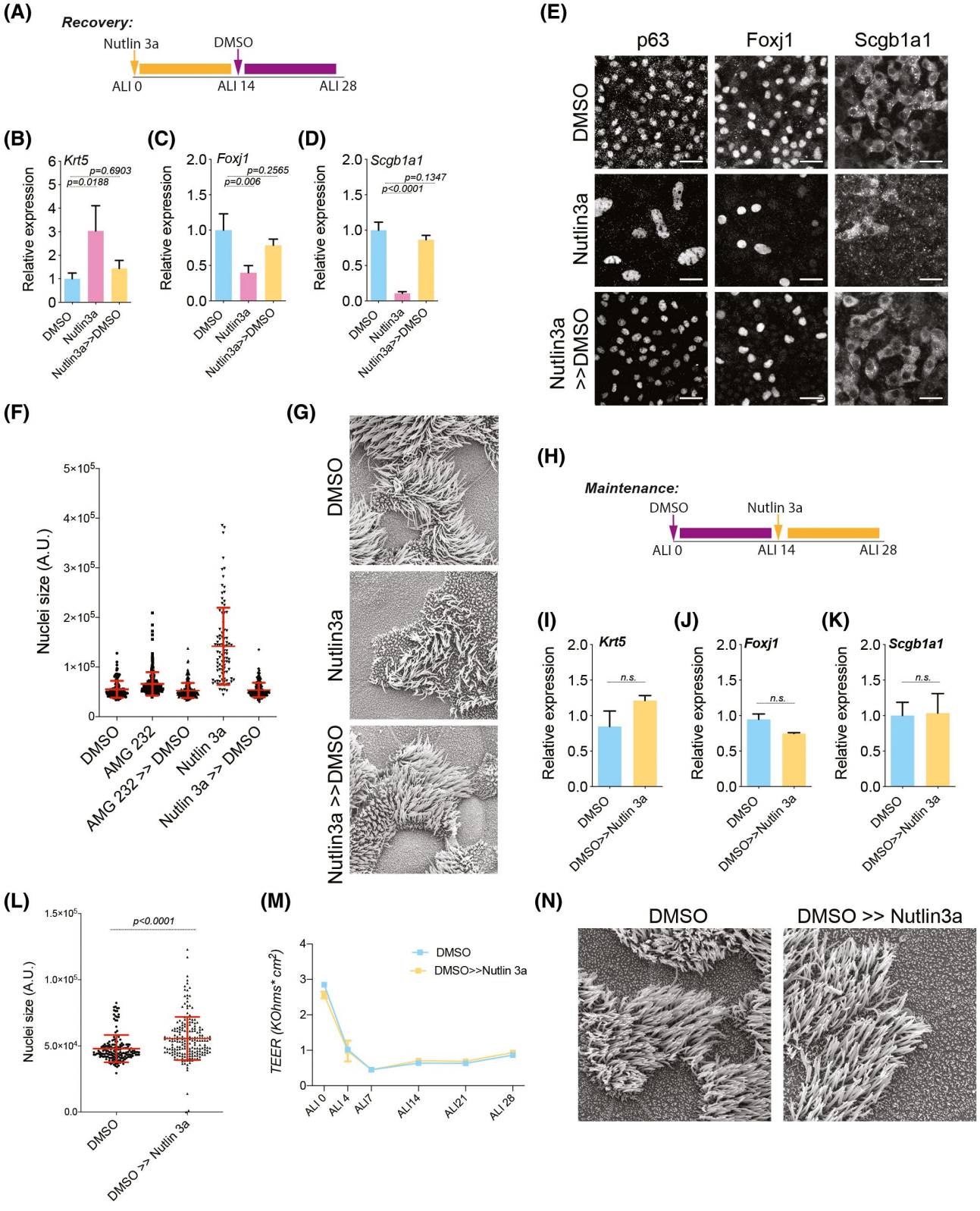

FIGURE 5 Nutlin-3a-induced phenotypes are completely reversible but do not affect cells once differentiated. A, Schematic representation of the recovery experiment. DMSO or Nutlin-3a was applied from ALI0 to ALI28 in a set of filters. In the recovery samples, Nutlin-3a was only applied from ALI0 to ALI14 and then from ALI14 to ALI28 DMSO was added (Nutlin-3a»DMSO). B-D, mRNA expression levels in cells treated with DMSO, Nutlin-3a, or Nutlin-3a»DMSO of Krt5 for basal cells (B), Foxj1 for MCCs (C), and Scgb1a1 for club cells (D). Mean relative to control cells (cells treated with DMSO for 28 days) and standard deviation as error bars were plotted for each lineage marker, n = 6. E, Representative images for DMSO, Nutlin-3a, and Nutlin-3a»DMSO cells processed for immunofluorescence to evaluate basal cells (p63), MCCs (Foxj1), and club cells (Scgb1a1). F, Quantification of nucleus size in DMSO, Nutlin-3a, and Nutlin-3a»DMSO experimental conditions, n > 100. G, Scanning electron micrographs of MTECs treated with DMSO, Nutlin-3a, or Nutlin-3a»DMSO. H, Schematic representation of the maintenance experiment. Cells were treated with DMSO for 28 days in a set of filters. In a parallel set of filters Nutlin-3a was added after 14 days in ALI. I-K, mRNA expression levels of Krt5 (I), Foxj1 (J), and Scgb1a1 (K) in the maintenance experiment. Mean relative to control cells (cells treated with DMSO for 28 days) and standard deviation as error bars were plotted for each lineage marker, n = 8. L, Quantification of nucleus size in DMSO and DMSO»Nutlin-3a experimental conditions, n > 200. M, Transepithelial electrical resistance (TEER) of MTECs treated with DMSO and DMSO»Nutlin-3a. N, Scanning electron micrographs of MTECs treated with DMSO, and DMSO»Nutlin-3a. Scale bar in E represents 20 μm. *P* values in all conditions were obtained using two-tailed *t* test

Nutlin-3a. As expected, we did not find a major effect on apoptosis or senescence (Figure S6). However, we found a 10%-20% increase in the percentage of cells in G1/G0 cell cycle phase in p53-KD cells or in Nutlin-3a-treated cells (Figure 6H). At the molecular level, we detected a Cyclin D1 protein increase only in Nutlin-3a-treated cells but not in p53-KD DMSO cells (Figure 6I,J).

Taken together these data indicates that p53 controls the self-renewal of BSCs, at least in part through cell cycle regulation, and that Nutlin-3a treatment in BSCs induced an accumulation of Cyclin D1, which is not observed in p53-KD DMSO cells.

3.7 | MDM2/p53 regulates BSCs differentiation on human airway epithelial cells

Looking at the expression level of MDM2, TP53, TP63, and TP73 in human airway epithelial cells using a published single-cell RNA-seq dataset, we found that, like in mice, MDM2 expression is enriched in MCCs (FOXN4+ and Ciliated cells) while TP53 expression is more homogeneously expressed (Figure S6F). Based on this information, we decided to test if MDM2/p53 role is recapitulated in human airway epithelial cells by looking at BSCs differentiation, epithelial integrity, and self-renewal. We started by assessing the role of the MDM2/p53 pathway in airway differentiation in BSCs isolated and expanded from two healthy donors (BRO 001 and BRO 002). We treated primary human airway epithelial cells along the differentiation process (21 days in ALI) with Nutlin-3a or DMSO. Analyses of the cell type-specific gene markers reveled that MDM2 inhibition cause a decrease in Foxj1 expression, supporting a reduction in MCCs like in mouse airway cells (Figure 7A,B). However, we found an increase in *Scgb1a1* and *Spdef* gene expression, indicating an increase in CCs and GCs (Figure 7A,B). SEM of the human airway monolayers treated with Nutlin-3a or DMSO confirmed the reduction of MCCs in Nutlin-3a-treated cells (Figure 7H,I). Those images also showed that in MDM2 inhibited some ciliated cells still develop and that the morphology of those cilia was not affected (Figure 7H,I). In terms of monolayer development and integrity, we observed a pseudostratified epithelium, with nuclei at different heights in DMSO or Nutlin-3a-treated cells (Figure 7E) and that Nutlin-3a treatment of human airway epithelial cells does not affect TEER (Figure 7C,D). Nevertheless, like in mouse airway cells, Nutlin-3a affects the epithelial monolayer cell density when nucleus size and number were measured (Figure 7E-G). Lastly, by looking at AOs size, we found that Nutlin-3a also affect BSCs self-renewal in human bronchial epithelial cells (Figure 7J), reproducing the phenotype observed in mouse airway epithelial cells.

Altogether, we could recapitulate the majority of the phenotypes observed in mouse airway when we block p53 degradation by MDM2 in human airway. We also found a major difference on the secretory differentiation phenotype, where Nutlin-3a caused a dramatic increase on secretory cells in human samples and the opposite in mouse airway.

4 | DISCUSSION

Airway regeneration in response to pathogens and pollutant is a well-coordinated process of various cellular events, including proliferation and differentiation. Here we established p53 as a key regulator of BSCs proliferation and differentiation and propose that p53 protein acts transiently during BSCs differentiation in a process regulated by MDM2 (Figure 7J). The p53 transcription factor family (p53, p63, and p73) plays a critical role during airway development. Both p63 and p53 knockout (KO) mice developed lung defects and p73 KO mice have respiratory disfunction.[12,14] In the trachea, cell composition is affected by removal of either p73 that increase CCs, or p63 that increases ciliated cells.[15] Although the mechanisms for p63 and p73 function on airway epithelial are well established, the role for p53 remained partially unknown. It has been previously reported that p53 is key regulator of airway epithelial cell density and composition

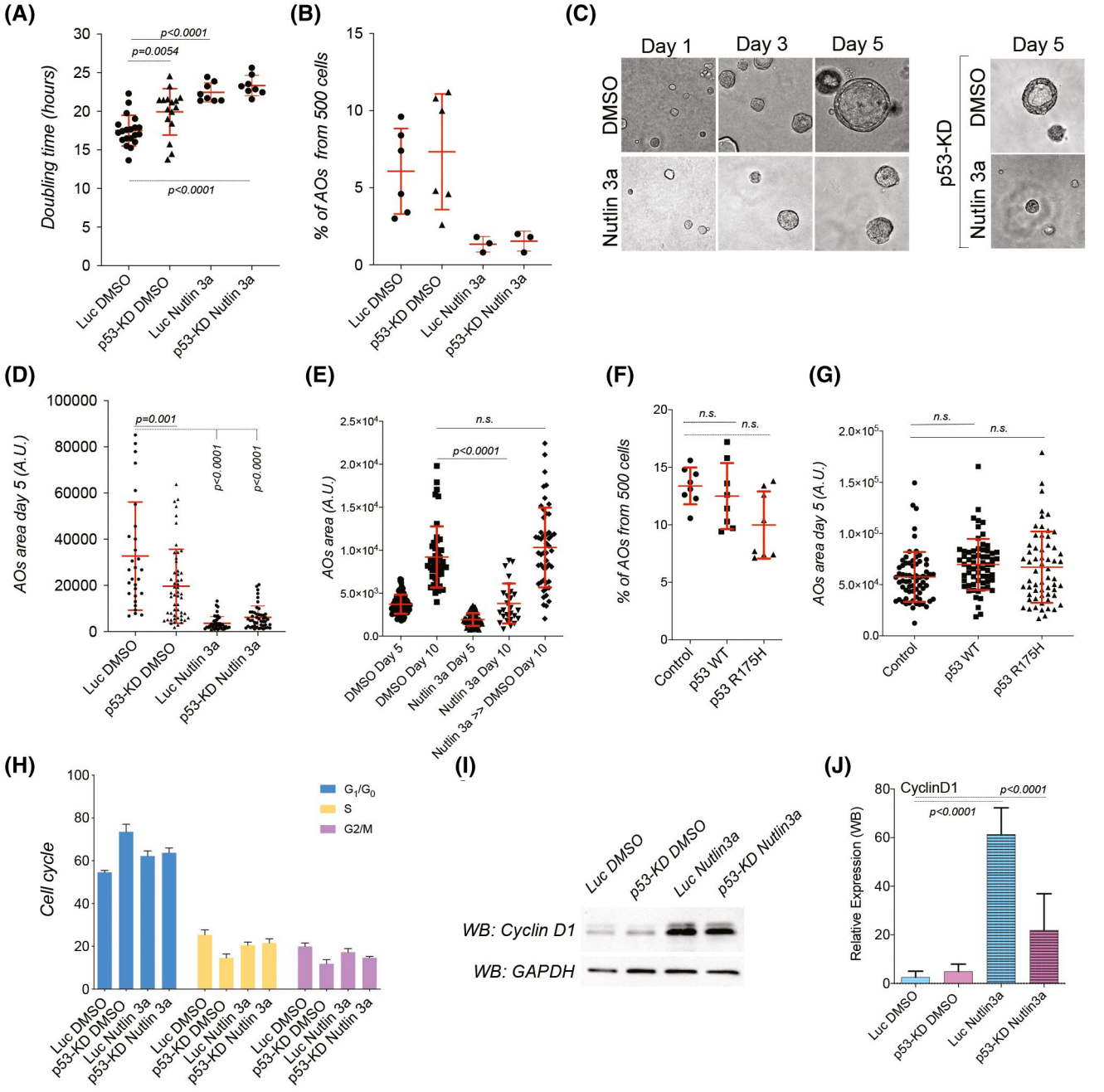

FIGURE 6 p53/MDM2 interaction is important for BSCs to proliferate. A, Quantification of the doubling time in control (Luc) or p53-KD MTECs treated with Nutlin-3a or DMSO (n = 6-14). B, Percentage of airway organoids (AOs) obtained in control (Luc) or p53-KD MTECs treated with Nutlin-3a or DMSO for 5 days (n = 3-6). C-E, Representative images of AOs development (C) and size quantification (D) in Luc or p53-KD cells treated with DMSO or Nutlin-3a. E, Quantification of AOs size in DMSO, Nutlin-3a, and Nutlin-3a»DMSO experimental conditions, n > 50. F, Percentage of airway organoids (AOs) obtained in control, p53 WT overexpressing cells, or p53 R175H overexpressing cells in day 5 after plating in matrigel (n = 8). G, Quantification of AOs size in control, p53 WT overexpressing cells, or p53 R175H overexpressing cells, n > 60. H, Cell cycle analyses in Luc or p53-KD cells treated with Nutlin-3a or DMSO for 5 days. I, Western blots images for Cyclin D1 and GAPDH in Luc or p53-KD cells treated with Nutlin-3a or DMSO. J, Quantification of Cyclin D1 WB protein levels. GAPDH was used as a loading control and then all values for each differentiation set were made relative to Luc DMSO. Mean and standard deviation as error bars were plotted, n = 4. *P* values in all conditions were obtained using two-tailed *t* test

through a mechanism that controls proliferation and differentiation when club progenitor cells were used as a source to develop the airway epithelia. Since p53 is a reprogramming barrier and regeneration from club progenitor cells requires a de-differentiation process, we decided to study the role of p53 directly on BSCs in differentiation. We found that p53 protein levels but not RNA levels change along the differentiation process, which is concomitant with a dramatic MDM2

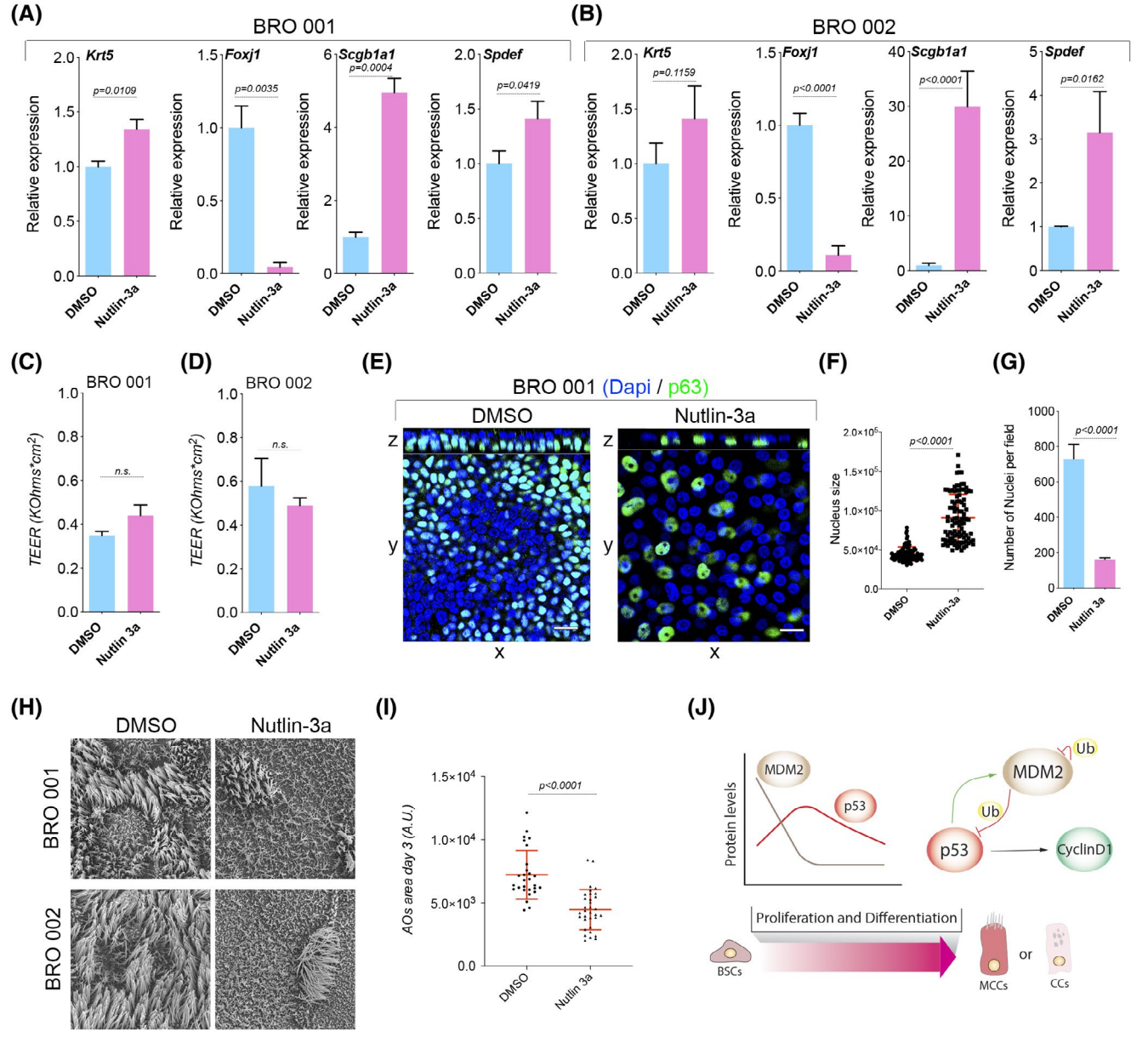

FIGURE 7 p53/MDM2 interaction is important for BSCs to proliferate. A,B, mRNA expression levels in human bronchial epithelial cells from donor BRO 001 (A) and BRO 002 (B). Cultures were treated until ALI21 with DMSO or Nutlin-3a. The expression of *Krt5* was used for basal cells, *Foxj1* for MCCs, *Scgb1a1* for club cells, and *Spdef* for goblet cells. C,D, Transepithelial electrical resistance (TEER) of human cells at ALI21 treated with DMSO or Nutlin-3a of BRO 001 (C) and BRO 002 (D). E, Representative immunofluorescence images for BRO 001 in ALI21 staining DAPI and P63 in DMSO and Nutlin-3a experimental conditions. F, Quantification of nucleus size in BRO 001, n > 100. G, Nuclei density in BRO 001. H, Representative scanning electron micrographs of human cultures in DMSO and Nutlin-3a treatments in ALI21. I, Quantification of AOs size in DMSO and Nutlin-3a at day 3, n > 30. J, Schematic representation showing the p53 and MDM2 function during airway differentiation. MDM2 regulates p53 protein levels during airway differentiation, most likely through ubiquitination. This mechanism is important to keep appropriate cell proliferation and differentiation from BSCs to MCCs and club cells (CCs). Scale bar in E represents 20 μm. *P* values in all conditions were obtained using two-tailed *t* test

downregulation at both RNA and protein levels. This is in agreement with previous data where changes on p53 RNA and protein levels occurs during mESC differentiation and mouse development in vivo.[40-42] The different roles of p53 in BSCs compared to CCs[16] might be explained by the MDM2 function, as MDM2 expression in CCs is very low. Moreover, direct inhibition of the MDM2/p53 interaction, a process by which p53 levels are increased, blocks the differentiation process in BSCs. This is an exception to the general view of p53 in stem cell biology, where in undifferentiated mESCs or iPSCs, the re-expression of p53 or activation drives them toward a more differentiated state.[42-44]

We also described that MDM2 protein varies along the differentiation process. Recently, it has been shown that

epithelium-specific inactivation of *Mdm2* led to lethality at birth with a reduction of lung size, which is reversible upon p53 removal. In contradiction with our data, they found that all the appropriate epithelial cell types were presented, including Foxj1- and Scgb1a1-positive cells.[45] This can be explained by a compensatory mechanism that are absent in our more acute model system. Furthermore, at this point we cannot abandon the idea that MDM2 could have additional functions independently of p53 in differentiated MCCs. There are recent examples for MDM2 function in cell differentiation. For example, MDM2 knockdown blocks adipocytes differentiation independent of p53 through regulation of the STAT family of transcription factors.[46] In mesenchymal stem cells, MDM2 supports the maintenance of stemness, and its removal promotes differentiation in a p53-independent manner.[47] In addition, NUMB, a negative regulator of Notch signaling, is also a known interactor for MDM2.[48,49]

Interestingly, most of the phenotypes observed in mouse were recapitulated when we used a human primary cell model, with the exception of a different outcome for secretory cells after MDM2 inhibition. These results suggest that the pharmacological modulation of p53 protein levels using MDM2/p53 interaction inhibitor would not dramatically affect the epithelial monolayer and that the observed phenotypes could be reversed upon drug removal. We hypothesize that MDM2 inhibition induced a reversible quiescent state in BSCs by increasing p53 and Cyclin D1. These findings could have potential medical implications since MDM2 inhibition has been demonstrated to be a plausible strategy to treat several cancer types including non-small cell lung cancer (NSCLC), where 40% are squamous cell carcinomas and express BSCs cell lineage markers Krt5, Sox2, and p63 as biomarkers. Furthermore, p53 mutation is the most frequent genetic alteration found in lung squamous cell carcinoma (SCC), present in about 79% of the cases,[50,51] and MDM2 has been found to be overexpressed in many human tumors.[52] Thus, elucidating the MDM2 function on the airway epithelia is important to improve lung cancer treatment and to understand MDM2 connections with the p53 family of proteins. In addition, to understand and control how BSCs repopulate an airway denuded of epithelium by injury has considerable relevance in regenerative medicine, where bioengineered replacement of lungs by seeding cells into de-cellularized lungs could be a medical approach. Taken together, our findings could have profound implications for patients with lung cancer where the MDM2/p53 pathway is altered, but also for airway regenerative biology where the p53 pathway modulation could be employed to control the timing of differentiation or other bioengineered processes.

ACKNOWLEDGMENTS

The authors are grateful to all members of the Carvajal lab for helpful suggestions, comments, and discussions during the development and execution of the project. The authors want to particularly acknowledge the patients and the Biobank del Área de Salud de Badajoz for their collaboration. Flow cytometry, confocal microscopy, and scanning electron microscopy were performed at the UEX microscopy core facilities. J.M.C.-G. was recipient of a Ramón y Cajal contract (RYC-2015-17867). This work was supported by BFU2014-54699-P, BFU2017-85547-P grants from the Ministry of Economy, and IB18014 from Junta de Extremadura to J.M.C.-G. and GR15164 from Junta de Extremadura to F.C. S.G.-J. was a recipient of a Fellowship from the Universidad de Extremadura. S.D.-Ch. and C.M.M.-Q. were recipients of a Fellowship from Junta de Extremadura. All Spanish funding is co-sponsored by the European Union FEDER program.

CONFLICT OF INTEREST

The authors declare no competing financial interests.

AUTHOR CONTRIBUTIONS

S. Garrido-Jimenez, J.F. Barrera-Lopez, S. Diaz-Chamorro, and C.M. Mateos-Quiros performed all of the experiments. A.C. Roman designed and performed the data analysis. I. Rodriguez-Blanco and F.L. Marquez-Perez provided the human samples. F. Centeno and M.J. Lorenzo designed the experiments. J.M. Carvajal-Gonzalez designed the experiments, analyzed the data, and wrote the manuscript.

ORCID

Jose Maria Carvajal-Gonzalez https://orcid.org/0000-0001-6576-830X

REFERENCES

1. Cardoso WV. Molecular regulation of lung development. *Annu Rev Physiol*. 2001;63:471-494.
2. Rawlins EL, Hogan BLM. Epithelial stem cells of the lung: privileged few or opportunities for many? *Development*. 2006;133:2455-2465.
3. Warburton D, Perin L, Defilippo R, Bellusci S, Shi W, Driscoll B. Stem/progenitor cells in lung development, injury repair, and regeneration. *Proc Am Thorac Soc*. 2008;5(6):703-706.
4. Rock JR, Onaitis MW, Rawlins EL, et al. Basal cells as stem cells of the mouse trachea and human airway epithelium. *Proc Natl Acad Sci U S A*. 2009;106:12771-12775.
5. Hogan BLM, Barkauskas CE, Chapman HA, et al. Repair and regeneration of the respiratory system: complexity, plasticity, and mechanisms of lung stem cell function. *Cell Stem Cell*. 2014;15:123-138.
6. Yang Y, Riccio P, Schotsaert M, et al. Spatial-temporal lineage restrictions of embryonic p63+ progenitors establish distinct stem cell pools in adult airways. *Dev Cell*. 2018;44:752-761.e4.

7. Rawlins EL, Okubo T, Xue Y, et al. The role of Scgb1a1+ clara cells in the long-term maintenance and repair of lung airway, but not alveolar, epithelium. *Cell Stem Cell*. 2009;4:525-534.
8. Tata PR, Mou H, Pardo-Saganta A, et al. Dedifferentiation of committed epithelial cells into stem cells in vivo. *Nature*. 2013;503:218-223.
9. Bustamante-Marin XM, Ostrowski LE. Cilia and mucociliary clearance. *Cold Spring Harb Perspect Biol*. 2017;9(4):a028241.
10. Beers MF, Morrisey EE. The three R's of lung health and disease: repair, remodeling, and regeneration. *J Clin Invest*. 2011;121:2065-2073.
11. Vaidyanathan S, Salahudeen AA, Sellers ZM, et al. High-efficiency, selection-free gene repair in airway stem cells from cystic fibrosis patients rescues CFTR function in differentiated epithelia. *Cell Stem Cell*. 2020;26:161-171.e4.
12. Yang A, Schweitzer R, Sun D, et al. p63 is essential for regenerative proliferation in limb, craniofacial and epithelial development. *Nature*. 1999;398:714-718.
13. Daniely Y, Liao G, Dixon D, et al. Critical role of p63 in the development of a normal esophageal and tracheobronchial epithelium. *Am J Physiol Cell Physiol*. 2004;287:C171-C181.
14. Nemajerova A, Kramer D, Siller SS, et al. TAp73 is a central transcriptional regulator of airway multiciliogenesis. *Genes Dev*. 2016;30:1300-1312.
15. Marshall CB, Mays DJ, Beeler JS, et al. P73 is required for multiciliogenesis and regulates the Foxj1-associated gene network. *Cell Rep*. 2016;14:2289-2300.
16. McConnell AM, Yao C, Yeckes AR, et al. p53 regulates progenitor cell quiescence and differentiation in the airway. *Cell Rep*. 2016;17:2173-2182.
17. Jeong Y, Hoang NT, Lovejoy A, et al. Role of KEAP1/NRF2 and TP53 mutations in lung squamous cell carcinoma development and radiation resistance. *Cancer Discov*. 2017;7:86-101.
18. You Y, Richer EJ, Huang T, Brody SL. Growth and differentiation of mouse tracheal epithelial cells: selection of a proliferative population. *Am J Physiol Lung Cell Mol Physiol*. 2002;283:L131 5-L1321.
19. Woo AJ, Patry CAA, Ghamari A, et al. Zfp281 (ZBP-99) plays a functionally redundant role with Zfp148 (ZBP-89) during erythroid development. *Blood Adv*. 2019;3:2499-2511.
20. Plasschaert LW, Žilionis R, Choo-Wing R, et al. A single-cell atlas of the airway epithelium reveals the CFTR-rich pulmonary ionocyte. *Nature*. 2018;560:377-381.
21. Barkauskas CE, Chung MI, Fioret B, Gao X, Katsura H, Hogan BLM. Lung organoids: current uses and future promise. *Development*. 2017;144:986-997.
22. Hogan B, Tata PR. Cellular organization and biology of the respiratory system. *Nat Cell Biol*. 2019:1.
23. Montoro DT, Haber AL, Biton M, et al. A revised airway epithelial hierarchy includes CFTR-expressing ionocytes. *Nature*. 2018;560:319-324.
24. Haupt Y, Maya R, Kazaz A, Oren M. Mdm2 promotes the rapid degradation of p53. *Nature*. 1997;387:296-299.
25. Kubbutat MHG, Jones SN, Vousden KH. Regulation of p53 stability by Mdm2. *Nature*. 1997;387:299-303.
26. Honda R, Tanaka H, Yasuda H. Oncoprotein MDM2 is a ubiquitin ligase E3 for tumor suppressor p53. *FEBS Lett*. 1997;420:25-27.
27. Chen J, Lin J, Levine AJ. Regulation of transcription functions of the p53 tumor suppressor by the mdm-2 oncogene. *Mol Med*. 1995;1:142-152.
28. Junk DJ, Vrba L, Watts GS, Oshiro MM, Martinez JD, Futscher BW. Different mutant/wild-type p53 combinations cause a spectrum of increased invasive potential in nonmalignant immortalized human mammary epithelial cells. *Neoplasia*. 2008;10:450-461.
29. Li L, Li X, Tang Y, Lao Z, Lei J, Wei G. Common cancer mutations R175H and R273H drive the p53 DNA-binding domain towards aggregation-prone conformations. *Phys Chem Chem Phys*. 2020;22:9225-9232.
30. Fischer M. Census and evaluation of p53 target genes. *Oncogene*. 2017;36:3943-3956.
31. Vassilev LT, Vu BT, Graves B, et al. In vivo activation of the p53 pathway by small-molecule antagonists of MDM2. *Science*. 2004;303:844-848.
32. Her NG, Oh JW, Oh YJ, et al. Potent effect of the MDM2 inhibitor AMG232 on suppression of glioblastoma stem cells. *Cell Death Dis*. 2018;9:1–12.
33. Sun D, Li Z, Rew Y, et al. Discovery of AMG 232, a potent, selective, and orally bioavailable MDM2-p53 inhibitor in clinical development. *J Med Chem*. 2014;57:1454-1472.
34. Pardo-Saganta A, Tata PR, Law BM, et al. Parent stem cells can serve as niches for their daughter cells. *Nature*. 2015;523:597-601.
35. Gravotta D, Carvajal-Gonzalez JM, Mattera R, et al. The clathrin adaptor AP-1A mediates basolateral polarity. *Dev Cell*. 2012;22:811-823.
36. Carvajal-Gonzalez JM, Gravotta D, Mattera R, et al. Basolateral sorting of the coxsackie and adenovirus receptor through interaction of a canonical YXXΦ motif with the clathrin adaptors AP-1A and AP-1B. *Proc Natl Acad Sci U S A*. 109; 2012:3820-3825.
37. Vousden KH, Prives C. Blinded by the light: the growing complexity of p53. *Cell*. 2009;137:413-431.
38. Marión RM, Strati K, Li H, et al. A p53-mediated DNA damage response limits reprogramming to ensure iPS cell genomic integrity. *Nature*. 2009;460:1149-1153.
39. Jain AK, Barton MC. p53: emerging roles in stem cells, development and beyond. *Development*. 2018;145:1–10.
40. Lin T, Chao C, Saito S, et al. p53 induces differentiation of mouse embryonic stem cells by suppressing Nanog expression. *Nat Cell Biol*. 2005;7:165-171.
41. Rogel A, Popliker M, Webb CG, Oren M. p53 cellular tumor antigen: analysis of mRNA levels in normal adult tissues, embryos, and tumors. *Mol Cell Biol*. 1985;5:2851-2855.
42. Sabapathy K, Klemm M, Jaenisch R, Wagner EF. Regulation of ES cell differentiation by functional and conformational modulation of p53. *EMBO J*. 1997;16:6217-6229.
43. Komarov PG, Komarova EA, Kondratov RV, et al. A chemical inhibitor of p53 that protects mice from the side effects of cancer therapy. *Science*. 1999;285:1733-1737.
44. Lee D-F, Su J, Ang Y-S, et al. Regulation of embryonic and induced pluripotency by aurora kinase-p53 signaling. *Cell Stem Cell*. 2012;11:179-194.
45. Sui P, Li R, Zhang Y, et al. E3 ubiquitin ligase MDM2 acts through p53 to control respiratory progenitor cell number and lung size. *Development*. 2019;146:1–7.
46. Hallenborg P, Siersbæk M, Barrio-Hernandez I, et al. MDM2 facilitates adipocyte differentiation through CRTC-mediated activation of STAT3. *Cell Death Dis*. 2016;7(6):e2289.
47. Wienken M, Dickmanns A, Nemajerova A, et al. MDM2 associates with polycomb repressor complex 2 and enhances stemness-promoting chromatin modifications independent of p53. *Mol Cell*. 2016;61:68-83.

48. Colaluca IN, Tosoni D, Nuciforo P, et al. NUMB controls p53 tumour suppressor activity. *Nature*. 2008;451:76-80.
49. Juven-Gershon T, Shifman O, Unger T, Elkeles A, Haupt Y, Oren M. The Mdm2 oncoprotein interacts with the cell fate regulator numb. *Mol Cell Biol*. 1998;18:3974-3982.
50. Hollstein M, Sidransky D, Vogelstein B, Harris CC. p53 mutations in human cancers. *Science*. 1991;253:49-53.
51. Chen Z, Fillmore CM, Hammerman PS, Kim CF, Wong KK. Non-small-cell lung cancers: a heterogeneous set of diseases. *Nat Rev Cancer*. 2014;14:535-546.
52. Momand J, Jung D, Wilczynski S, Niland J. The MDM2 gene amplification database. *Nucleic Acids Res*. 1998;26:3453-3459.

SUPPORTING INFORMATION

Additional Supporting Information may be found online in the Supporting Information section.

How to cite this article: Garrido-Jimenez S, Barrera-Lopez JF, Diaz-Chamorro S, et al. p53 regulation by MDM2 contributes to self-renewal and differentiation of basal stem cells in mouse and human airway epithelium. *FASEB J*. 2021;35:e21816. https://doi.org/10.1096/fj.202100638R